

See discussions, stats, and author profiles for this publication at: <https://www.researchgate.net/publication/326952322>

Transport and retention of silver nanoparticles in soil: Effects of input concentration, particle size and surface coating

Article in *Science of The Total Environment* · August 2018

CITATIONS

0

READS

689

3 authors:



Jianzhou He

Michigan State University

10 PUBLICATIONS 120 CITATIONS

[SEE PROFILE](#)



Dengjun Wang

United States Environmental Protection Agency

56 PUBLICATIONS 690 CITATIONS

[SEE PROFILE](#)



Dong-Mei Zhou

Chinese Academy of Sciences

263 PUBLICATIONS 5,946 CITATIONS

[SEE PROFILE](#)

Some of the authors of this publication are also working on these related projects:



Fate and Transport of Nanohybrids in the Subsurface [View project](#)



environmental science [View project](#)



Transport and retention of silver nanoparticles in soil: Effects of input concentration, particle size and surface coating

Jianzhou He^{a,b}, Dengjun Wang^c, Dongmei Zhou^{a,*}

^a Key Laboratory of Soil Environment and Pollution Remediation, Institute of Soil Science, Chinese Academy of Sciences, Nanjing 210008, China

^b University of Chinese Academy of Sciences, Beijing 100049, China

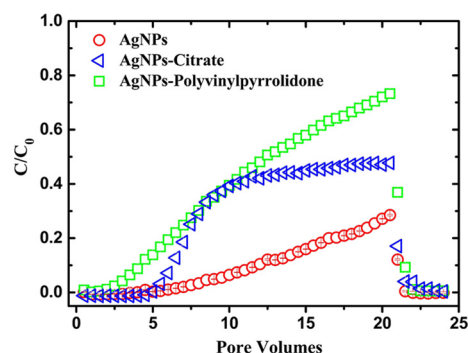
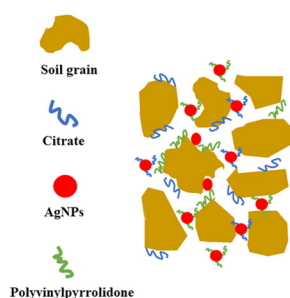
^c National Research Council Resident Research Associate, U.S. Environmental Protection Agency, Ada, OK 74820, United States



HIGHLIGHTS

- Migration of AgNPs in the Ultisol was low due to high surface area and retention sites.
- Increased transport occurred at higher particle concentration and smaller particle size.
- Surface coatings promoted AgNPs transport by effectively blocking the solid-phase sites.
- The 1- or 2-species model successfully described the behaviors of AgNPs in soil columns.

GRAPHICAL ABSTRACT



ARTICLE INFO

Article history:

Received 14 June 2018

Received in revised form 9 August 2018

Accepted 10 August 2018

Available online 11 August 2018

Editor: Xinbin Feng

Keywords:

Silver nanoparticles

Soil

Transport

Surface coating

Numerical model

ABSTRACT

Soils are considered as a major sink for engineered nanoparticles (ENPs) because of their inevitable release to the subsurface environment during production, transportation, use and disposal processes. In this context, the transport and retention of silver nanoparticles (AgNPs) with different input particle concentration, particle size, and surface coating were investigated in clay loam using water-saturated column experiments. Our results showed that the mobility of AgNPs in the soil was considerably low, and >73.9% of total injected AgNPs (except for no coating condition) was retained in columns. This is primarily due to the high specific surface area and favorable retention sites in soil. Increased transport of AgNPs occurred at higher input concentration and smaller particle size. The presence of surface coatings (i.e., polyvinylpyrrolidone (PVP) and citrate) further promoted the transport and reduced the retention of AgNPs in soil, which is likely due to their effective blocking of the solid-phase sites that are originally available for AgNPs retention. Although the shape of retention profiles (RPs) of AgNPs was either hyperexponential or nonmonotonic that is different from the colloid filtration theory prediction, the 1-species (consider both time- and depth-dependent retention) and/or 2-species (account for the release of reversibly deposited AgNPs) model successfully described the transport behaviors of AgNPs in soil columns under all the investigated conditions. This study proves the applicability of mathematical model in predicting the fate and transport of ENPs in real soils, and our findings presented herein are significant to ultimately develop management strategies for reducing the potential risks of groundwater contamination due to ENPs entering the environment.

© 2018 Elsevier B.V. All rights reserved.

* Corresponding author.

E-mail address: dmzhou@issas.ac.cn (D. Zhou).

1. Introduction

After over 20 years of basic and applied research, nanotechnology is undergoing rapid development and industrialization. The overall market value of products incorporating nanotechnology is projected to be about \$3 trillion by the year of 2020 (Roco, 2011). Engineered nanoparticles (ENPs) are increasingly incorporated into many industrial and consumer products. According to the Consumer Products Inventory (CPI), currently there are 1814 consumer products in 32 countries (Vance et al., 2015) in a wide range, such as textile, paint, clothing, sunscreen, cosmetics, antimicrobial agents, medicine, food additives, pesticides, etc. (Council NR, 2012; Kah et al., 2013; Kah and Hofmann, 2014). In particular, silver nanoparticles (AgNPs) are the most frequently used nanomaterial type, accounting for 435 products (or 24%) of the total nanomaterials produced (Vance et al., 2015). With the increasing application of AgNPs environmental seepage are inevitable, which may occur through multiple pathways, such as atmospheric deposition, irrigation with wastewater effluent, land application of sewage sludge, and stormwater runoff (Gardea-Torresdey et al., 2014; Gottschalk et al., 2009; Klaine et al., 2008; Wiesner et al., 2006). The released AgNPs would eventually enter the major repository, that is, soil. In this regard, a thorough understanding of the fate and transport of AgNPs in soils is of critical significance for their benign use, risk assessment, and waste management.

During the last decade, most of the research on the fate and transport of AgNPs were performed using well-defined model porous media (e.g., quartz sand and glass bead) (El Badawy et al., 2013; Liang et al., 2013b; Lin et al., 2011; Mitzel and Tufenkji, 2014; Tian et al., 2010). While natural soils are highly complex and heterogeneous with respect to their physicochemical characteristics, such as varied soil pH, soil organic matter (SOM) and cation exchange capacity, mineral composition and specific surface area, broad grain size distribution, as well as complex pore structure (Wang et al., 2014a, 2014b, 2015). For example, AgNPs dissolution was only detected in 6 soils of 16 soil suspensions with a wide range of physicochemical properties, which was possibly attributed to the strong partitioning of dissolved Ag^+ ions to soil grains (median $K_d = 1791 \text{ L kg}^{-1}$) (Cornelis et al., 2012). Moreover, the partitioning process became more significant predominantly with increased SOM content. X-ray microtomography analysis suggested that AgNPs transport in natural soil was strongly influenced by soil aggregate size (Sagee et al., 2012). And they found that chemical interactions between AgNPs and soil grains were of pivotal importance as a retention mechanism. Retained AgNPs were strongly associated with soil colloids composed of Si, Fe, Al, and organic matters (Makselon et al., 2018). Therefore, information obtained from those studies in model porous media may have limited applicability for predicting the fate and transport of AgNPs in natural soils (Cornelis et al., 2012, 2013; Darlington et al., 2009; Jaisi and Elimelech, 2009; Sagee et al., 2012; Yopasá Arenas et al., 2018). In addition, most AgNPs incorporated into commercial products are typically modified with capping agents, such as ligands (e.g., citrate) and polymers (e.g., polyvinylpyrrolidone, PVP). These coatings are thought to strongly affect the surface chemistries, subsequently, impact on their mobility, reactivity, and toxicity in natural environments (El Badawy et al., 2011, 2012; Levard et al., 2012).

Laboratory column experiments were conducted to systematically investigate the effects of input particle concentration, particle size, and surface coating on the transport and retention of AgNPs in soil, which was a complement to our previous work (Wang et al., 2014a) examining effects of soil grain size, solution ionic strength and composition, flow rate, and capping agent concentration. Again, attempts were made to better understand the mechanisms behind AgNPs mobility using 1-species and/or 2-species transport model. The overall goal of this study is to deepen our current knowledge of key physicochemical factors controlling the fate and transport of AgNPs in real subsurface environments (i.e., soil and sediment).

2. Materials and methods

2.1. Chemicals

Deionized water (resistivity: $18.2 \text{ M}\Omega \text{ cm}$, Milli-Q, Millipore, USA) was utilized for preparing all aqueous solutions. Analytical reagent-grade KNO_3 , AgNO_3 and citric acid were obtained from Sinopharm Chemical Reagent Co., Ltd. (Shanghai, China). Biotech-grade PVP (MW = $40,000 \text{ g mol}^{-1}$) was purchased from Biosharp (Hefei, China).

2.2. Soil

Surface soil (0–20 cm) was sampled from the Ecological Experiment Station of Red Soil, Chinese Academy of Sciences (Yujiang County, Jiangxi, China). Prior to use, the soil was air-dried, gently ground, and sieved to obtain median grain size of $650 \mu\text{m}$ (soil size distribution of 600–710 μm). The soil was classified as clay loam with 30% sand, 43% silt, and 27% clay. Additional properties were documented in our previous publications (Wang et al., 2014a; Wang et al., 2014b) and also retrieved in Supporting Information (SI) Table S1. Briefly, this soil had a pH of 4.6, organic matter content of 6.6 g kg^{-1} , cation exchange capacity of 8.5 cmol kg^{-1} , and a specific surface area of $24 \text{ m}^2 \text{ g}^{-1}$. The clay fraction consisted of kaolinite, montmorillonite and hydromica. The surface charge of the soil in 1 mM KNO_3 solution was determined to be $-15.0 \pm 1.1 \text{ mV}$ using a NanoBrook 90Plus PALS apparatus (Brookhaven Instruments, USA).

2.3. AgNPs suspensions

Silver nanoparticles (AgNPs) with two different sizes were used in this study. Commercial AgNPs (denoted as small AgNPs) were purchased from the Nanjing XFANO Materials Tech Co., Ltd. (Nanjing, China). In-house AgNPs (denoted as large AgNPs) were synthesized as per Yu et al. (2014) method with a slight modification, details were described in the Supporting Information Text S1. AgNPs stocks were stored at $4 \text{ }^\circ\text{C}$ in the dark before use. Aliquots of AgNPs stock solution were transferred into 1 mM KNO_3 electrolyte solution containing 0.5% PVP or 0.5% citrate. Subsequently, the mixture of AgNPs with 0.5% PVP/citrate coating was vigorously stirred for 1 h, followed by sonication for 30 min prior to the column transport experiments. The pH value of AgNPs solutions was unbuffered and ranged between 4.5 and 5.3.

The scanning spectra of small and large AgNPs were obtained using an UV-Vis spectrophotometer (UV-2700, Shimadzu corporation, Japan) at the wavelength ranging from 200 to 800 nm. Their zeta potentials and hydrodynamic diameters (D_h) were examined with NanoBrook 90Plus PALS analyzer (Brookhaven, USA) at room temperature. Morphological images of AgNPs were taken using a transmission electron microscope (TEM, JEM-2100, Japan), in which particle size distribution was calculated using Nanomeasurer 1.2 software based on randomly selected ~100 particles from 10 TEM images.

2.4. Column transport experiments

Transport experiments were performed in duplicates using glass chromatography column with 1.2-cm inner diameter and 10-cm in length. Both ends of column were capped with polytetrafluoroethylene and stainless-steel mesh (80- μm opening) to support the packed bed. The vertically-oriented columns were dry-packed by carefully adding 1–2 cm increments of soil grains ($650 \mu\text{m}$) followed by gentle vibration to eliminate any layering (Wang et al., 2012a). The packed height was around 8.5 cm. A well-established procedure of saturating and conditioning the packed column was applied to stabilize the soil colloids and to avoid pore clogging (Wang et al., 2014a, 2014b, 2015). Detailed protocol was stated in SI Text S2. A nonreactive tracer (bromide) experiment was performed to obtain the fluid pore-water velocity and

dispersion coefficient of packed columns, which were then used for numerical simulations of AgNPs transport (described in Section 2.5).

Afterwards, three sets of column experiments were conducted to examine the roles of particle properties in the transport and retention of AgNPs in soil. The first set investigated the input AgNPs concentrations ($C_0 = 2.5, 5.0, 10 \text{ mg L}^{-1}$) with the presence of 0.5% PVP acting as a stabilizer. Secondly, the effect of particle sizes (size = 15.0 and 27.4 nm) on the transport of AgNPs in soil was examined. The third set explored different surface coatings (i.e., PVP and citrate). The experimental ionic strength and flow rate were maintained constantly at 1.0 mM KNO_3 and 0.25 mL min^{-1} , respectively. For each set of experiment, the AgNPs suspensions of interest were injected into the column using a peristaltic pump (YZIT-15, Baoding Longer Precision Pump Co., Ltd., China) for 20 pore volumes (PVs), followed by elution with background electrolyte (1.0 mM KNO_3) until a low and stable absorbance signal was obtained. Meanwhile, the AgNPs suspension was continuously stirred with a magnetic stirrer to disperse the AgNPs at the duration of experiments. It should be mentioned that very limited dissolution (<3%) of AgNPs occurred over the time frame of transport experiments (Wang et al., 2014a). So, the dissolution effect was deemed to be negligible in this study. The AgNPs effluents were regularly collected using a fraction collector (BS-100A, Huxi Analytical Instrument Factory Co., Ltd., China) and immediately determined with UV-Vis spectrophotometer (UV-2700, Shimadzu corporation, Japan) at a wavelength of 400 nm to quantify AgNPs concentrations (SI Text S3 and Fig. S1).

After the completion of each column experiment, the soil grain in the column was carefully excavated in 1-cm increment (8 layers). The soil segment was dried in an oven at $85 \text{ }^\circ\text{C}$, then ground and digested by HNO_3 -HF acids. Total Ag in the digestion was measured with inductively coupled plasma-atomic emission spectroscopy (ICP-AES, PerkinElmer, US). Finally, the mass balance was calculated based on the mass of AgNPs in the effluents, retained in soil, and the total injected amount.

2.5. Mathematical model

In this study, the one-dimensional convection–dispersion equation (CDE) coded in CXTFIT (Toride et al., 1999) was used to evaluate the fluid pore-water velocity and dispersion coefficient by fitting tracer breakthrough curves (BTCs). The 1-species or 2-species model was applied to describe the observed BTCs and retention profiles (RPs), i.e., hyperexponential and nonmonotonic) of AgNPs in soil. The HYDRUS-1D code (Simunek et al., 2008) was used to numerically evaluate the transport parameters of AgNPs by inverse fitting to the experimental BTCs and RPs with a non-linear least square optimization routine based on the Levenberg–Marquardt algorithm (Marquardt, 1963).

When experimental RPs were hyperexponential shape, a single mobile species (i.e., species 1) is considered, and the aqueous and solid-phase mass balance equations for AgNPs are given as (Bradford et al., 2006):

$$\frac{\partial(\theta_w C_1)}{\partial t} = -\nabla J_1 - \theta_w \psi_{block} k_1 C_1 + \rho_b k_{1det} S_1 \quad (1)$$

$$\frac{\partial(\rho_b S_1)}{\partial t} = \theta_w \psi_{block} k_1 C_1 - \rho_b k_{1det} S_1 \quad (2)$$

where θ_w is the volumetric water content [–], C_1 is the AgNPs concentration in aqueous phase of species 1 [M L^{-3} ; where M and L denote units of mass and length, respectively], t is the time [T; where T denotes the unit of time], J_1 is the total solute flux for species 1 [$\text{N L}^{-2} \text{T}^{-1}$; where N denotes number], ρ_b is the soil bulk density [M L^{-3}], S_1 is the solid-phase concentration of species 1 [N M^{-1}], k_1 and k_{1det} are the first-order deposition and detachment rate coefficient for species 1 [T^{-1}], respectively, and ψ_{block} is a dimensionless function to account for both time and depth-dependent retention for species 1 [–]. When ψ_{block}

= 1, an exponential distribution of AgNPs is predicted with depth (Yao et al., 1971). Nonetheless, ψ_{block} can be < 1 when it is given as (Bradford et al., 2006; Liang et al., 2013a):

$$\psi_{block} = \left(1 - \frac{S_1}{S_{max1}}\right) \left(\frac{d_{50} + z}{d_{50}}\right)^{-\beta_1} \quad (3)$$

where β_1 is an empirical parameter controlling the shape of the spatial distribution of AgNPs for species 1 [–], d_{50} is the medium grain size of porous media [L], S_{max1} is the maximum solid-phase concentration of AgNPs for species 1 [N M^{-1}], and z is the down gradient distance from the column inlet [L]. The first term on the right hand of Eq. (3) describes time-dependent deposition according to the Langmuirian approach (Adamczyk et al., 1994). This term implies that deposition decreases with time and that RP becomes uniform with depth as S_1 approaches S_{max1} (Liang et al., 2013a). The second term on the right hand of Eq. (3) is used to account for depth dependent deposition, that is, a decreasing deposition rate with depth. Note that when $\beta_1 = 0$, this term goes to 1, and an exponential distribution of AgNPs is predicted with depth. Conversely, when $\beta_1 > 1$ is employed, then the RP of AgNPs exhibits a hyperexponential shape (i.e., a higher deposition rate adjacent to the column inlet) (Bradford et al., 2003).

The above 1 species model can describe time dependent BTCs and RPs that are exponential, uniform, or hyperexponential with depth, but is not applicable for nonmonotonic RPs (i.e., a peak in particle deposition down-gradient from the column inlet) that have been observed in this study. Hence, a release term is incorporated in Eq. (2) to account for observed nonmonotonic RPs, which produces a second reversibly retained species (i.e., species 2) at a different rate than species 1. In this case, the mass balance equations for species 1 and 2 of AgNPs are given as (Bradford et al., 2006):

$$\frac{\partial(\theta_w C_1)}{\partial t} = -\nabla J_1 - \theta_w \psi_{block} k_1 C_1 + \rho_b k_{1det} S_1 \quad (4)$$

$$\frac{\partial(\rho_b S_1)}{\partial t} = \theta_w \psi_{block} k_1 C_1 - \rho_b k_{1det} S_1 - \rho_b k_{12} F_p \quad (5)$$

$$\frac{\partial(\theta_w C_2)}{\partial t} = -\nabla J_2 - \theta_w k_2 C_2 + \rho_b k_{2det} S_2 + \rho_b k_{12} F_p \quad (6)$$

$$\frac{\partial(\rho_b S_2)}{\partial t} = \theta_w k_2 C_2 - \rho_b k_{2det} S_2 \quad (7)$$

where the subscript 2 on $C, J,$ and S denotes the reversible species 2, k_{12} is the first-order production rate coefficient to account for the release rate of reversibly deposited AgNPs into the aqueous phase [T^{-1}], k_2 and k_{2det} are the first-order deposition and detachment rate coefficient for species 2 [T^{-1}], respectively, and F_p is the production function for species 2 [N M^{-1}]. It is assumed that a critical value (S_{crit1}) of S_1 needs to be reached before deposited AgNPs can be released into the aqueous phase ($F_p > 0$). The value of F_p is therefore defined as the maximum of $(S_1 - S_{crit1})$ and 0, where S_{crit1} is the critical concentration of S_1 when reversible deposition starts [N M^{-1}]. For values of $S_1 < S_{crit1}$, no release of deposited AgNPs occurs, and $F_p = 0$ (Bradford et al., 2006).

3. Results and discussion

3.1. Properties of AgNPs suspensions

The UV-Vis scanning spectra and TEM images of the small and large AgNPs used in this study are presented in Figs. S2 and 1, respectively. The maximum absorption peak of small AgNPs is more uniformly distributed, and the half peak width is narrower, in comparison to that of large AgNPs, indicating that the particle size distribution of small AgNPs is narrower and the uniformity is better. The TEM images showed that the AgNPs exhibited monodisperse; small AgNPs were

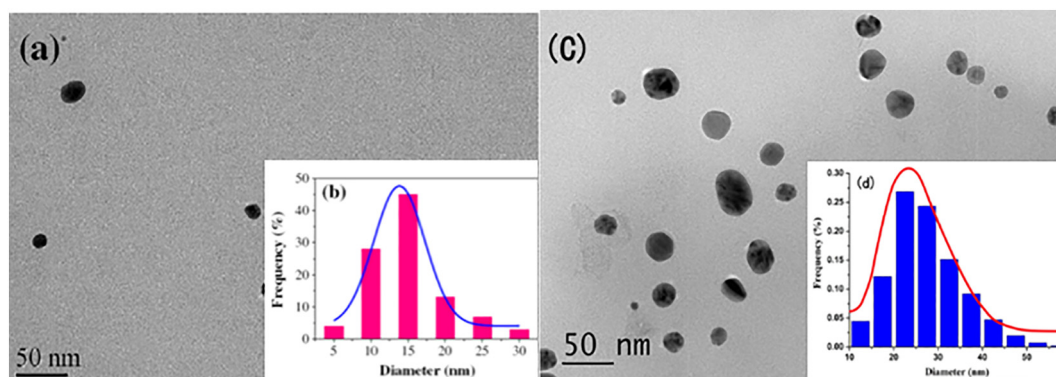


Fig. 1. Representative TEM images (a, c) and particle size distribution (b, d) of small (a, b) and large (c, d) AgNPs. Figure (a, b) is cited from Wang et al. (2014a). Copyright: 2014 Elsevier.

spherical-shaped with a homogeneous distribution, and large AgNPs mostly showed irregular shape and an uneven particle size. The calculated TEM particle sizes were 15.0 ± 3.6 nm (Wang et al., 2014a) for small AgNPs and 27.4 ± 8.2 nm for large AgNPs, respectively.

Table 1 gives the zeta potentials and hydrodynamic diameters (D_h) of AgNPs at various solution chemistries. The D_h value of AgNPs without surface coating was measured at 106 nm, which is much larger than their TEM size (15.0 nm), indicative of AgNPs aggregates for D_h measurements. Surface coatings (i.e., PVP and citrate) can greatly affect the electrokinetic properties of AgNPs. The presence of PVP increased the zeta potential of AgNPs from -24.9 mV to -11.8 mV, consistent with the results in the literature (Wang et al., 2014a). The D_h of small AgNPs decreased from 106 nm to 63.9 nm when 0.5% PVP was added, due to the dominant role of steric repulsion in inhibiting AgNPs aggregation (El Badawy et al., 2012; Thio et al., 2012). Conversely, large AgNPs with a smaller D_h (45.7 nm) was observed, which can be partially explained by the more negative zeta potential (-13.9 mV) of large AgNPs suspension with the addition of 0.5% PVP. Citrate slightly decreased the aggregation of AgNPs via repulsive electrostatics (El Badawy et al., 2012; Thio et al., 2012), as the zeta potential of AgNPs declined to -26.7 mV in the presence of 0.5% citrate.

3.2. Effect of particle concentration

When TEM size = 15.0 nm and surface coating = 0.5% PVP, the observed and simulated BTCs and RPs of AgNPs with various input particle concentrations ($C_0 = 2.5, 5.0,$ and 10 mg L $^{-1}$) are plotted in Fig. 2. The normalized effluent concentration (C/C_0) of AgNPs increased in response to the increase of input concentration (C_0); the higher C_0 , the steeper slope of BTC (Fig. 2a). This concentration-dependent transport behavior of AgNPs can be reasonably explained by blocking effect (Bradford and Bettahar, 2006), that is, attachment sites are occupied rapidly over time at higher C_0 . Liang et al. (2013b) observed shape transition of RPs from hyperexponential to nonmonotonic, and then to uniform when C_0 was increased from 1 to 5, and then to 10 mg L $^{-1}$. They attributed the development of nonmonotonic RPs for time-dependent blocking (Liang et al., 2013b). Similar results have also been reported

Table 1
Summary of column experimental parameters and electrokinetic properties of AgNPs suspensions.

AgNPs (mg L $^{-1}$)	TEM size (nm)	Coatings	D_h (nm)	Zeta potential (mV)
2.5	15.0	0.5% PVP	65.8	-11.8
5.0	15.0	0.5% PVP	63.0	-11.8
10	15.0	0.5% PVP	63.9	-11.8
10	27.4	0.5% PVP	45.7	-13.9
10	15.0	0.5% PVP	63.9	-11.8
10	15.0	0.5% Citrate	104	-26.7
10	15.0	No coating	106	-24.9

in other publications (Kasel et al., 2013; Sun et al., 2015). Input particle concentrations exerted significant effect on the shape of RPs. Nonmonotonic distributions of retained AgNPs were observed (Fig. 2b). Particularly, the depth of deposition peaks in the nonmonotonic RPs increased as particle concentrations increased. For example, as $C_0 = 2.5$ mg L $^{-1}$, the peak depth was 4 cm from the column inlet, whereas it increased to 8 cm when $C_0 = 10$ mg L $^{-1}$ of AgNPs, suggesting greater down-gradient mobility of AgNPs with higher concentration. In our previous paper (Wang et al., 2014a), nonmonotonic RPs of PVP-AgNPs were also obtained in a wide range of physicochemical factors (i.e., soil grain size, ionic strength and composition, flow rate, and PVP concentration).

Table 2 provides the summary of mass recovery of transport experiments and 1- and 2-species model-fitted parameters of k_1 , $S_{\max 1}/C_0$, $S_{\text{crit}1}$, k_{12} , k_2 , $k_{2\text{det}}$, and correlation coefficients (R^2). Soils are highly complicated and heterogeneous in terms of physicochemical characteristics, moreover, the AgNPs concentrations were quantified using two different methods (UV-Vis and ICP-AES for quantifications of AgNPs in column effluents and retentates, respectively), which altogether will likely cause minor errors in calculating the mass recovery of AgNPs in this study. Nevertheless, relatively high mass balance ($M_{\text{tot}} = 79.4\%$ – 101%) was obtained (except for the one without surface coating; $M_{\text{tot}} = 58.7\%$; Table 2), which is in accordance with the findings in our previous work (Wang et al., 2014a).

While not all (100%) of AgNPs were recovered, judging from $R^2 > 0.93$, the 1-species (for hyperexponential case) or 2-species (for nonmonotonic case) model still successfully described the BTCs and RPs of AgNPs under different investigated conditions in this study. For example, a huge difference of $S_{\max 1}/C_0$ values between different tested conditions (e.g., pre-treat PVP vs. pre-treat citrate vs. no coating) was observed, suggesting that the model-fitted parameters can be used to reliably explain AgNPs transport mechanisms in soils (while M_{tot} was not high). The values of deposition rate coefficient for species 1 (k_1) increased linearly with increasing particle concentration (C_0), meanwhile, the values of critical solid-phase concentration for species 1 ($S_{\text{crit}1}$) were reversibly related with C_0 , indicating a time-dependent retention (Liang et al., 2013b; Wang et al., 2014a). At the highest input concentration (10 mg L $^{-1}$), the solid-phase migration of AgNPs approach the lowest $S_{\text{crit}1}$ value (8.3×10^{-3} cm 3 g $^{-1}$) while at the highest deposition rate k_1 (0.33 min $^{-1}$), apparently, the time for blocking those retention sites is less. Hence, a rapid increase of BTC and a much deeper down-gradient migration of RP simultaneously occurred at input concentration of 10 mg L $^{-1}$ (Fig. 2 and Table 2). In addition, for species 2, the deposition rate coefficients (k_2) were remarkably larger than detachment rate coefficients ($k_{2\text{det}}$), resulting in more than 78.5% of applied AgNPs were retained in soil columns (Table 2). Consequently, the mobility of AgNPs in the soil was considerably lower than that observed in glass bead- and quartz sand-packed columns (Liang et al., 2013b; Lin et al., 2011). The retained AgNPs level reached the highest concentration of

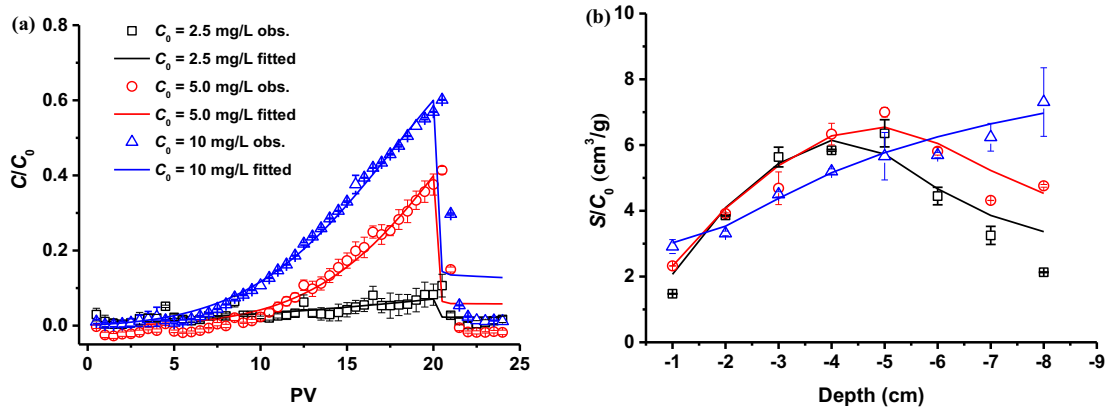


Fig. 2. Observed and simulated BTCs (a) and RPs (b) for AgNPs at different input concentrations (C_0). The BTCs are plotted as normalized effluent concentration (C/C_0) of AgNPs as a function of PVs. The RPs are plotted as normalized solid-phase concentration (S/C_0) versus depth from the column inlet. Open symbols are experimental data and solid lines are fitted results using the 2-species model since nonmonotonic RPs occur. Error bars represent the standard deviations in duplicate experiments.

199.5 mg/kg soil for large AgNPs with 0.5% PVP surface coating in the present work, which was about 10-fold higher than reported solid-phase concentrations of AgNPs on sand (Liang et al., 2013b). This is likely due to the high specific surface area and favorable sites of the soil for AgNPs retention (Wang et al., 2014a). Negatively charged AgNPs were preferentially retained by positively charged edges of clay minerals and Fe oxides (Cornelis et al., 2012; Wang et al., 2014a). Makselon et al. (2017, 2018) and Zhang et al. (2017) provided strong evidence that the retention and remobilization of AgNPs and CNT in soil were highly associated with soil colloids.

3.3. Effect of particle size

When $C_0 = 10$ mg L⁻¹ and surface coating = 0.5% PVP, the observed and simulated BTCs and RPs of AgNPs with two different particle sizes (15.0 and 27.4 nm) are presented in Fig. 3. Negligible amounts (0.21%) of large AgNPs (27.4 nm) were detected in the effluents, while the effluent concentration of small AgNPs (15.0 nm) increased over time, achieving the maximum C/C_0 of 0.61. These results agree with previous findings (Litton and Olson, 1996; Pelley and Tufenkji, 2008). Noticeably, the RPs of AgNPs were significantly different. Hyperexponential shape with 81.8% of AgNPs retained near the column inlet (1–3 cm) was observed for large AgNPs (27.4 nm), by contrast, nonmonotonic deposition of small AgNPs (15.0 nm) was noticed with the peak depth at 8 cm. We speculated that quite different RPs are related to the inherent size (i.e., TEM size). Since larger AgNPs tend to experience a rapid sedimentation due to strong gravitational force effect (Yao et al., 1971), they are expected to have higher mass transfer rate from the aqueous phase to the solid phase (collector surface). Additionally, chemical heterogeneity of soil grains can partially explain the hyperexponential RP of larger AgNPs because of stronger interaction between more negatively

charged larger AgNPs and positive edges of clay and iron oxides (Wang et al., 2014a).

The hyperexponential and nonmonotonic RPs of AgNPs were simulated using the 1-species ($R^2 = 0.97$) and 2-species model ($R^2 = 0.99$), respectively (Fig. 3b and Table 2). The value of $S_{\max 1}/C_0$ for large AgNPs (27.4 nm) was 1.2×10^5 cm³ g⁻¹, which was 3-order of magnitude larger than for small AgNPs (15.0 nm, $S_{\max 1}/C_0 = 224$ cm³ g⁻¹). The fitted results suggested that large AgNPs cannot completely occupy the retention sites adjacent to the column inlet, consequently, hyperexponential RP is expected to occur (Bradford et al., 2011; Wang et al., 2014a).

3.4. Effect of surface coating

When $C_0 = 10$ mg L⁻¹ and TEM size = 15.0 nm, the observed and simulated BTCs and RPs of AgNPs with different surface coatings (i.e., PVP and citrate) are shown in Fig. 4. PVP and citrate enhanced the transport and reduced the retention of AgNPs in soil columns to different extents. Without surface coating, the maximum C/C_0 was 0.29, and this increased to 0.61 and 0.45 in the presence of PVP and citrate, respectively. The enhanced transport of AgNPs by PVP is likely due to the steric repulsion preventing AgNPs approach to soil surface (El Badawy et al., 2012; Thio et al., 2012). The presence of citrate promoted the mobility of AgNPs can be explained by the repulsive electrostatics as zeta potential of AgNPs slightly decreased with the addition of 0.5% citrate (Table 1).

Many studies (Wang et al., 2012b, 2014c) have revealed that capping agents (e.g., PVP and citrate) were not only grafted on the ENPs surface, but also freely remained in the suspension. In this study, the freely-existed PVP and citrate are expected to preferentially adsorb onto the soil grains, thereby impairing the overall available sites for

Table 2

Mass recovery of column transport experiments, and fitted parameters based on 1-species and 2-species models.

AgNPs (mg L ⁻¹)	TEM size (nm)	Coatings	k_1 (min ⁻¹)	$S_{\max 1}/C_0$ (cm ³ g ⁻¹)	$S_{\text{crit}1}$ (cm ³ g ⁻¹)	k_{12} (min ⁻¹)	k_2 (min ⁻¹)	$k_{2\text{det}}$ (min ⁻¹)	R^2	M_{eff}	M_{ret}	M_{tot}
2.5	15.0	0.5% PVP	0.10	23.8	0.1	0.91	41.3	0.39	0.96	2.02	78.5	80.5
5.0	15.0	0.5% PVP	0.15	12.8	0.01	2.9×10^{-3}	35.7	0.40	0.97	2.78	83.7	86.5
10	15.0	0.5% PVP	0.33	224	8.3×10^{-3}	5.9×10^{-1}	23.0	0.78	0.99	2.72	80.9	83.6
10	27.4	0.5% PVP	0.31	1.2×10^5	NA	NA	NA	NA	0.97	0.21	90.6	90.8
10	15.0	0.5% PVP	0.33	224	8.3×10^{-3}	0.59	23.0	0.78	0.99	2.72	80.9	83.6
10	15.0	Pre-treat PVP	0.28	187	7.3×10^{-3}	0.04	21.6	0.69	0.98	5.45	73.9	79.4
10	15.0	0.5% Citrate	0.20	2.0×10^5	NA	NA	NA	NA	0.95	2.79	98.4	101
10	15.0	Pre-treat Citrate	0.24	1.3×10^5	NA	NA	NA	NA	0.93	3.04	87.5	90.5
10	15.0	No coating	0.12	26.4	9.06×10^{-3}	1.0×10^{-3}	36.3	0.45	0.97	1.16	57.5	58.7

k_1 is the first-order deposition rate coefficient for species 1; $S_{\max 1}$ is the maximum solid-phase concentration of AgNPs for species 1; $S_{\text{crit}1}$ is a critical value of solid-phase concentration of species 1; k_{12} is the first-order production rate coefficient; k_2 and $k_{2\text{det}}$ are the first-order deposition and detachment rate coefficient for species 2, respectively; R^2 is the squared regression coefficient; M_{eff} , M_{ret} , and M_{tot} are the mass percentages of AgNPs in the effluents, retained in soil and total, respectively; NA denotes not applicable.

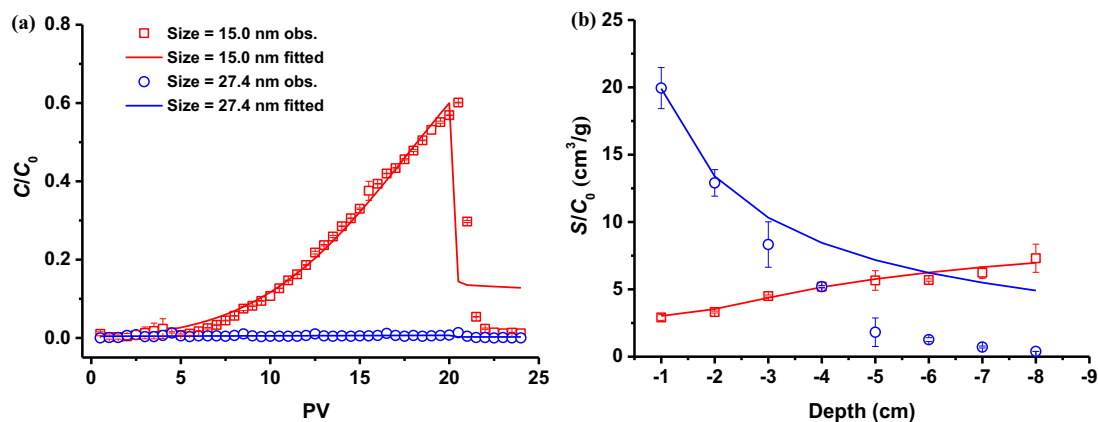


Fig. 3. Observed and simulated BTCs (a) and RPs (b) for AgNPs with different particle sizes. The BTCs are plotted as normalized effluent concentration (C/C_0) of AgNPs as a function of PVs. The RPs are plotted as normalized solid-phase concentration (S/C_0) versus depth from the column inlet. Open symbols are experimental data and solid lines are model results. The hyperexponential and nonmonotonic RPs of AgNPs were fitted using the 1-species and 2-species model, respectively. Error bars represent the standard deviations in duplicate experiments.

AgNPs retention. To evaluate the role of surface coatings (i.e., PVP and citrate), either freely existed in aqueous solution or loosely associated with nanoparticle, in the transport and retention of AgNPs in soil, additional experiments were carried out under the same solution chemistry did before, except that the column was pre-conditioned with 3 PVs of 0.5% PVP or 0.5% citrate solution before injection of AgNPs influents. The results clearly demonstrated that free aqueous PVP and citrate further increased the breakthrough of AgNPs resulting in higher mass recovery in the effluents ($M_{eff} = 5.45\%$ for PVP and $M_{eff} = 3.04\%$ for citrate, respectively) (Fig. 4 and Table 2). These results imply that PVP/citrate can effectively block the solid-phase sites that are originally available for AgNPs retention (Liang et al., 2013b; Wang et al., 2014a; Wang et al., 2014c). This finding is in good agreement with Wang et al. (2014c) study. They found that residual polyacrylic acid-octylamine polymer preferentially adsorbed onto the Ottawa sand surface near the column inlet, thereby preventing quantum dots attachment.

Again, 1-species or 2-species model accurately fitted BTCs and RPs of AgNPs with varying coatings (Fig. 4 and Table 2). Interestingly, the shape of RPs was nonmonotonic for PVP tests, differed from the hyperexponential-shaped RPs for citrate (Fig. 4b). The different shapes of RPs can also be explained by the time-dependent retention of AgNPs. The S_{max1}/C_0 value was $\sim 10^5$ in 0.5% citrate, AgNPs cannot fully fill these retention sites of solid surface, thus hyperexponential RPs were obtained. Compared to citrate, the S_{max1}/C_0 for PVP was 3-order

of magnitude smaller, which was occupied rapidly, thereby yielding the nonmonotonic RPs.

4. Conclusions

In this work, the effects of input particle concentration, particle size, and surface coating on the transport and retention of AgNPs in soil-packed columns were systematically examined. The mobility of AgNPs increased with increasing input particle concentration and decreasing particle size. The shapes of AgNPs RPs were sensitive to the investigated experimental conditions. The observed nonmonotonic RPs can be explained by the time-dependent retention and the down-gradient migration of AgNPs was increased in response to the increase of input concentration. The presence of surface coatings promoted the transport and reduced the retention of AgNPs in soil, which is likely due to the effective blocking of the solid-phase sites that are originally available for AgNPs retention. Note that the migration of AgNPs was considerably low and >73.9% of the injected AgNPs (except for no coating condition) were retained in soil columns. Most importantly, the experimental BTCs and RPs of AgNPs were successfully described using 1-species and 2-species models in this study. It should be mentioned that in this research, complemented our previous work (Wang et al., 2014a, 2015), clearly elucidated that the transport behavior of AgNPs in natural soils was extremely complicated, which was jointly determined by the physicochemical properties of soil, pore-water solution, NP, as well as

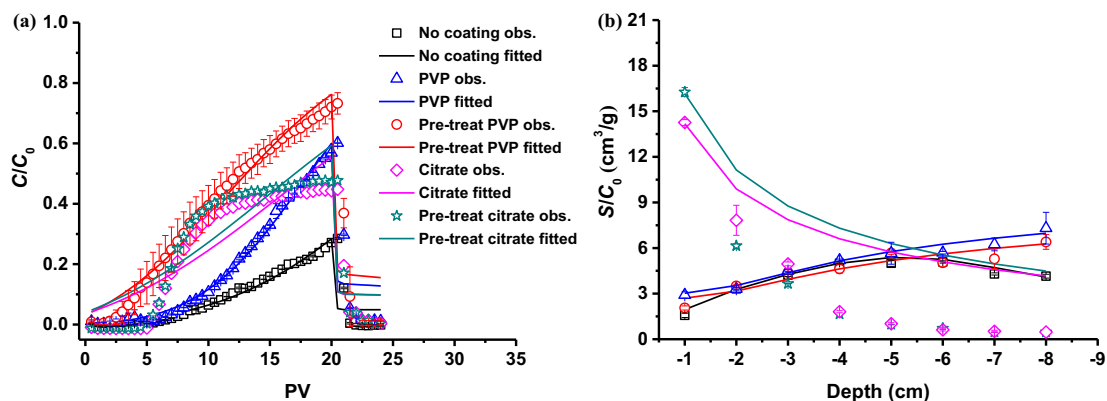


Fig. 4. Observed and simulated BTCs (a) and RPs (b) for AgNPs with different surface coatings. The BTCs are plotted as normalized effluent concentration (C/C_0) of AgNPs as a function of PVs. The RPs are plotted as normalized solid-phase concentration (S/C_0) versus depth from the column inlet. Open symbols are experimental data and solid lines are model results. The hyperexponential and nonmonotonic RPs of AgNPs were fitted using the 1-species and 2-species model, respectively. Error bars represent the standard deviations in duplicate experiments.

hydrodynamics. And the capping agents (e.g., PVP and citrate) greatly increased the mobility and thus potential risks of AgNPs migration down to the groundwater. Fortunately, the mathematical model is applicable and promising to predict ENPs' fate and transport in real soil. The modelling outcomes will greatly help us expedite the prediction of potential risks of ENPs in complicated subsurface environments like soils and sediments.

Acknowledgments

This work was supported by the National Natural Science Foundation of China (projects Nos. 41430752 and 41125007) and the National Basic Research and Development Program of China (project No. 2013CB934303).

Appendix A. Supplementary data

Supplementary data to this article can be found online at <https://doi.org/10.1016/j.scitotenv.2018.08.136>.

References

- Adamczyk, Z., Siwek, B., Zembala, M., Belouschek, P., 1994. Kinetics of localized adsorption of colloid particles. *Adv. Colloid Interf. Sci.* 48, 151–280.
- Bradford, S.A., Bettahar, M., 2006. Concentration dependent transport of colloids in saturated porous media. *J. Contam. Hydrol.* 82, 99–117.
- Bradford, S.A., Simunek, J., Bettahar, M., van Genuchten, M.T., Yates, S.R., 2003. Modeling colloid attachment, straining, and exclusion in saturated porous media. *Environ. Sci. Technol.* 37, 2242–2250.
- Bradford, S.A., Simunek, J., Walker, S.L., 2006. Transport and straining of *E. coli* O157:H7 in saturated porous media. *Water Resour. Res.*, 42 <https://doi.org/10.1029/2005wr004805>.
- Bradford, S.A., Torkzaban, S., Simunek, J., 2011. Modeling colloid transport and retention in saturated porous media under unfavorable attachment conditions. *Water Resour. Res.* 47, W10503. <https://doi.org/10.1029/2011WR010812>.
- Cornelis, G., Doolettemadeleine Thomas, C., McLaughlin, M.J., Kirby, J.K., Beak, D.G., Chittleborough, D., 2012. Retention and dissolution of engineered silver nanoparticles in natural soils. *Soil Sci. Soc. Am. J.* 76, 891–902.
- Cornelis, G., Pang, L., Doolette, C., Kirby, J.K., McLaughlin, M.J., 2013. Transport of silver nanoparticles in saturated columns of natural soils. *Sci. Total Environ.* 463–464, 120–130.
- Council NR, 2012. A Research Strategy for Environmental, Health, and Safety Aspects of Engineered Nanomaterials. National Academies Press.
- Darlington, T.K., Neigh, A.M., Spencer, M.T., Guyen, O.T., Oldenburg, S.J., 2009. Nanoparticle characteristics affecting environmental fate and transport through soil. *Environ. Toxicol. Chem.* 28, 1191–1199.
- El Badawy, A.M., Aly Hassan, A., Scheckel, K.G., Suidan, M.T., Tolaymat, T.M., 2013. Key factors controlling the transport of silver nanoparticles in porous media. *Environ. Sci. Technol.* 47, 4039–4045.
- El Badawy, A.M., Scheckel, K.G., Suidan, M., Tolaymat, T., 2012. The impact of stabilization mechanism on the aggregation kinetics of silver nanoparticles. *Sci. Total Environ.* 429, 325–331.
- El Badawy, A.M., Silva, R.G., Morris, B., Scheckel, K.G., Suidan, M.T., Tolaymat, T.M., 2011. Surface charge-dependent toxicity of silver nanoparticles. *Environ. Sci. Technol.* 45, 283–287.
- Gardea-Torresdesy, J.L., Rico, C.M., White, J.C., 2014. Trophic transfer, transformation, and impact of engineered nanomaterials in terrestrial environments. *Environ. Sci. Technol.* 48, 2526–2540.
- Gottschalk, F., Sonderer, T., Scholz, R.W., Nowack, B., 2009. Modeled environmental concentrations of engineered nanomaterials (TiO₂, ZnO, Ag, CNT, fullerenes) for different regions. *Environ. Sci. Technol.* 43, 9216–9222.
- Jaisi, D.P., Elimelech, M., 2009. Single-walled carbon nanotubes exhibit limited transport in soil columns. *Environ. Sci. Technol.* 43, 9161–9166.
- Kah, M., Beulke, S., Tiede, K., Hofmann, T., 2013. Nanopesticides: state of knowledge, environmental fate, and exposure modeling. *Crit. Rev. Environ. Sci. Technol.* 43, 1823–1867.
- Kah, M., Hofmann, T., 2014. Nanopesticide research: current trends and future priorities. *Environ. Int.* 63, 224–235.
- Kasel, D., Bradford, S.A., Šimunek, J., Heggen, M., Vereecken, H., Klumpp, E., 2013. Transport and retention of multi-walled carbon nanotubes in saturated porous media: effects of input concentration and grain size. *Water Res.* 47, 933–944.
- Klaine, S.J., Alvarez, P.J., Batley, G.E., Fernandes, T.F., Handy, R.D., Lyon, D.Y., Mahendra, S., McLaughlin, M.J., Lead, J.R., 2008. Nanomaterials in the environment: behavior, fate, bioavailability, and effects. *Environ. Toxicol. Chem.* 27, 1825–1851.
- Levard, C., Hotze, E.M., Lowry, G.V., Brown, G.E., 2012. Environmental transformations of silver nanoparticles: impact on stability and toxicity. *Environ. Sci. Technol.* 46, 6900–6914.
- Liang, Y., Bradford, S.A., Simunek, J., Heggen, M., Vereecken, H., Klumpp, E., 2013a. Retention and remobilization of stabilized silver nanoparticles in an undisturbed loamy sand soil. *Environ. Sci. Technol.* 47, 12229–12237.
- Liang, Y., Bradford, S.A., Simunek, J., Vereecken, H., Klumpp, E., 2013b. Sensitivity of the transport and retention of stabilized silver nanoparticles to physicochemical factors. *Water Res.* 47, 2572–2582.
- Lin, S., Cheng, Y., Bobcombe, Y., L Jones, K., Liu, J., Wiesner, M.R., 2011. Deposition of silver nanoparticles in geochemically heterogeneous porous media: predicting affinity from surface composition analysis. *Environ. Sci. Technol.* 45, 5209–5215.
- Litton, G.M., Olson, T.M., 1996. Particle size effects on colloid deposition kinetics: evidence of secondary minimum deposition. *Colloids Surf. A Physicochem. Eng. Asp.* 107, 273–283.
- Makselon, J., Siebers, N., Meier, F., Vereecken, H., Klumpp, E., 2018. Role of rain intensity and soil colloids in the retention of surfactant-stabilized silver nanoparticles in soil. *Environ. Pollut.* 238, 1027–1034.
- Makselon, J., Zhou, D., Engelhardt, I., Jacques, D., Klumpp, E., 2017. Experimental and numerical investigations of silver nanoparticle transport under variable flow and ionic strength in soil. *Environ. Sci. Technol.* 51, 2096–2104.
- Marquardt, D., 1963. An algorithm for least-squares estimation of nonlinear parameters. *J. Soc. Ind. Appl. Math.* 11, 431–441.
- Mitzel, M.R., Tufenkji, N., 2014. Transport of industrial PVP-stabilized silver nanoparticles in saturated quartz sand coated with *Pseudomonas aeruginosa* PAO1 biofilm of variable age. *Environ. Sci. Technol.* 48, 2715–2723.
- Pelley, A.J., Tufenkji, N., 2008. Effect of particle size and natural organic matter on the migration of nano- and microscale latex particles in saturated porous media. *J. Colloid Interface Sci.* 321, 74–83.
- Roco, M.C., 2011. The long view of nanotechnology development: the National Nanotechnology Initiative at 10 years. *J. Nanopart. Res.* 13, 427–445.
- Sagee, O., Dror, I., Berkowitz, B., 2012. Transport of silver nanoparticles (AgNPs) in soil. *Chemosphere* 88, 670–675.
- Simunek, J., van Genuchten, M.T., Sejna, M., 2008. The HYDRUS-1D Software Package for Simulating the One-dimensional Movement of Water, Heat, and Multiple Solutes in Variably Saturated Media. Version 4.0. HYDRUS Software Series 3 Department of Environmental Science, University of California Riverside, Riverside, California.
- Sun, Y., Gao, B., Bradford, S.A., Wu, L., Chen, H., Shi, X., Wu, J., 2015. Transport, retention, and size perturbation of graphene oxide in saturated porous media: effects of input concentration and grain size. *Water Res.* 68, 24–33.
- Thio, B.J.R., Montes, M.O., Mahmoud, M.A., Lee, D.-W., Zhou, D., Keller, A.A., 2012. Mobility of capped silver nanoparticles under environmentally relevant conditions. *Environ. Sci. Technol.* 46, 6985–6991.
- Tian, Y., Gao, B., Silvera-Batista, C., Ziegler, K.J., 2010. Transport of engineered nanoparticles in saturated porous media. *J. Nanopart. Res.* 12, 2371–2380.
- Toride, N., Leij, F., Van Genuchten, M.T., 1999. The CXTFIT Code for Estimating Transport Parameters From Laboratory or Field Tracer Experiments. Vol. 2. Version 2.1, U.S. Salinity Laboratory, USDA-ARS, Riverside, California.
- Vance, M.E., Kuiken, T., Vejerano, E.P., McGinnis, S.P., Hochella Jr., M.F., Rejeski, D., Hull, M.S., 2015. Nanotechnology in the real world: redeveloping the nanomaterial consumer products inventory. *Beilstein Journal of Nanotechnology* 6, 1769.
- Wang, D., Bradford, S.A., Paradelo, M., Peijnenburg, W.J.G.M., Zhou, D., 2012a. Facilitated transport of copper with hydroxyapatite nanoparticles in saturated sand. *Soil Sci. Soc. Am. J.* 76, 375–388.
- Wang, D., Ge, L., He, J., Zhang, W., Jaisi, D.P., Zhou, D., 2014a. Hyperexponential and nonmonotonic retention of polyvinylpyrrolidone-coated silver nanoparticles in an Ultisol. *J. Contam. Hydrol.* 164, 35–48.
- Wang, D., Jaisi, D.P., Yan, J., Jin, Y., Zhou, D., 2015. Transport and retention of polyvinylpyrrolidone-coated silver nanoparticles in natural soils. *Vadose Zone J.* 14. <https://doi.org/10.2136/vzj2015.01.0007>.
- Wang, D., Su, C., Zhang, W., Hao, X., Cang, L., Wang, Y., Zhou, D., 2014b. Laboratory assessment of the mobility of water-dispersed engineered nanoparticles in a red soil (Ultisol). *J. Hydrol.* 519, 1677–1687.
- Wang, Y., Becker, M.D., Colvin, V.L., Abriola, L.M., Pennell, K.D., 2014c. Influence of residual polymer on nanoparticle deposition in porous media. *Environ. Sci. Technol.* 48, 10664–10671.
- Wang, Y., Li, Y., Costanza, J., Abriola, L.M., Pennell, K.D., 2012b. Enhanced mobility of fullerene (C₆₀) nanoparticles in the presence of stabilizing agents. *Environ. Sci. Technol.* 46, 11761–11769.
- Wiesner, M.R., Lowry, G.V., Alvarez, P., Dionysiou, D., Biswas, P., 2006. Assessing the Risks of Manufactured Nanomaterials. ACS Publications.
- Yao, K.M., Habibi, M.T., O'Melia, C.R., 1971. Water and waste water filtration: concepts and applications. *Environ. Sci. Technol.* 5, 1105–1112.
- Yopasa Arenas, A., de Souza, Pessôa G., Arruda, M.A.Z., Fostier, A.H., 2018. Mobility of polyvinylpyrrolidone coated silver nanoparticles in tropical soils. *Chemosphere* 194, 543–552.
- Yu, S., Yin, Y., Chao, J., Shen, M., Liu, J., 2014. Highly dynamic PVP-coated silver nanoparticles in aquatic environments: chemical and morphology change induced by oxidation of Ag⁰ and reduction of Ag⁺. *Environ. Sci. Technol.* 48, 403–411.
- Zhang, M., Bradford, S.A., Šimunek, J., Vereecken, H., Klumpp, E., 2017. Roles of cation valence and exchange on the retention and colloid-facilitated transport of functionalized multi-walled carbon nanotubes in a natural soil. *Water Res.* 109, 358–366.